The EMBO Journal vol.13 no.6 pp.1357-1367, 1994

Generation of interleukin-6 receptor antagonists by molecular-modeling guided mutagenesis of residues important for gp130 activation

Rocco Savino, Armin Lahm[1], Anna Laura Salvati, Laura Ciapponi, Elisabetta Sporeno, Sergio Altamura, Giacomo Paonessa, Carlo Toniatti and Gennaro Ciliberto[2]

Departments of Genetics and [1]Biocomputing, Istituto di Ricerche di Biologia Molecolare P.Angeletti (IRBM), Via Pontina Km 30, 600, 00040 Pomezia (Rome), Italy
[2]Corresponding author

Communicated by G.Ciliberto

Interleukin-6 (IL-6) drives the sequential assembly of a receptor complex formed by the IL-6 receptor (IL-6Rα) and the signal transducing subunit, gp130. A model of human IL-6 (hIL-6) was constructed by homology using the structure of bovine granulocyte colony stimulating factor. The modeled cytokine was predicted to interact sequentially with the cytokine binding domains of IL-6Rα and gp130 bridging them in a way similar to that of the interaction between growth hormone and its homodimeric receptor. Several residues on helices A and C which were predicted as contact points between IL-6 and gp130 and therefore essential for IL-6 signal transduction, were subjected to site-directed mutagenesis individually or in combined form. Interestingly, while single amino acid changes never produced major alterations in IL-6 bioactivity, a subset of double mutants of Y31 and G35 showed a considerable reduction of biological activity and were selectively impaired from associating with gp130 in binding assays *in vitro*, while they maintained wild-type affinity towards hIL6-Rα. More importantly, we demonstrated the antagonistic effect of mutant Y31D/G35F versus wild-type IL-6.

Key words: antagonist/gp130 interaction/interleukin-6/molecular modeling/mutagenesis

Introduction

Growth factors and cytokines exert their activity through interaction with specific receptors or receptor combinations. In most instances cytokines drive the sequential assembly of a multiprotein complex on the surface of target cells through the recruitment of more than one receptor molecule. In multiprotein receptor assembly processes the first step has the function of trapping the ligand on the cell surface and of generating a composite binding site which is required for the recruitment of other transmembrane components. In the most simple cases this process of receptor assembly is achieved through the homodimerization of single receptors such as the case of erythropoietin (Watowich *et al.*, 1992), growth hormone (GH) (Cunningham *et al.*, 1991; De Vos *et al.*, 1992), granulocyte colony stimulating factor (G-CSF) (Nagata and Fukunaga, 1991) and interferon-γ (Greenlund *et al.*, 1993) or through heterodimerization as observed for interleukin-3, granulocyte macrophage-colony stimulating factor (GM-CSF) and interleukin-5 (Miyajima *et al.*, 1993). In other examples, a heterotrimeric receptor complex is formed which requires the participation of three different molecules, as is the case of interleukin-2 (IL-2) (Takeshita *et al.*, 1992).

Deciphering the pathway of receptor complex formation and identifying the patches of amino acid residues on the ligand surface which are the driving force of this process are of fundamental importance both for understanding the mechanisms responsible for the activation of intracellular processes, and for the generation of ligand mimics with specific biological properties, such as receptor agonists or antagonists.

During the last few years a group of cytokines which has received considerable attention due to the peculiar properties of their complex receptor system is that constituted by interleukin-6 (IL-6), leukemia inhibitory factor, oncostatin M, ciliary neurotrophic factor and interleukin-11 (Kishimoto *et al.*, 1992; Taga and Kishimoto, 1992; Yin *et al.*, 1993). We will refer to this group as the IL-6 family. All these molecules presumably share structural similarities with each other and with several other growth factors like GH, interferon-β, IL-2, IL-4, IL-5, macrophage-colony stimulating factor (M-CSF), G-CSF and GM-CSF: a scaffold formed by a bundle of four α-helices linked by three loops of variable length (Bazan, 1990a). Interestingly, while each member of the IL-6 family assembles its own specific multiprotein receptor complex, one receptor is common to all of them, namely gp130 (Taga and Kishimoto, 1992; Taga *et al.*, 1992; Yin *et al.*, 1993). This receptor also plays a central role in activating intracellular processes (Hibi *et al.*, 1990; Taga *et al.*, 1992; Davis *et al.*, 1993), thus the constant recruitment and activation of gp130 explains the functional redundancy of the IL-6 family cytokines.

The best studied member of this family is IL-6. Physiologically IL-6 has been demonstrated as a growth and differentiation factor on various cell types, and as an inducer of acute phase gene expression in hepatocytes (Van Snick, 1990). Moreover, the dysregulation of IL-6 production has been invoked in the pathogenesis of autoimmune diseases (Hirano *et al.*, 1990; Kishimoto *et al.*, 1992), multiple myeloma (Suematsu *et al.*, 1986, 1992) and, more recently, post-menopausal osteoporosis (Jilka *et al.*, 1992).

IL-6 first interacts with the extracellular region of the IL-6 receptor (IL-6Rα) molecule on the surface of target cells (Yamasaki *et al.*, 1988; Taga *et al.*, 1989). A complex is formed which can then associate with gp130 (Taga *et al.*, 1989; Hibi *et al.*, 1990); neither IL-6 nor IL-6Rα alone can associate with gp130. As the intracytoplasmic and transmembrane domains of IL-6Rα do not play any essential role in intracellular signaling (Taga *et al.*, 1989; Fiorillo *et al.*, 1992b), a soluble form of IL-6Rα is thus an IL-6 agonist, because it is still able to form a complex with IL-6 in solution and thereafter to associate properly with gp130.

No structural information is available to date on either IL-6 or its receptors. It would, however, be extremely advantageous to get information about the molecular mechanisms of interaction between the three molecules, also because of the possibility of manipulating them to generate receptor antagonists for therapeutical purposes. Ideally, a possible receptor antagonist could be an IL-6 mutant which preserves its binding to IL-6Rα but is selectively unable to recruit gp130, thereby blocking the receptor in an 'inactive' configuration.

In order to gather information about this process we have developed a computer assisted three-dimensional model of the IL-6−IL-6Rα−gp130 interaction based on the structural similarities between these three molecules and the components of the GH receptor complex, whose structure has been resolved in detail by X-ray crystallography (De Vos *et al.*, 1992). Besides the aforementioned similarities between GH and IL-6, both IL-6 receptors contain a typical cytokine binding domain (CBD), whose global fold is believed to reproduce that present in the GH receptor (Bazan, 1990b). By analogy with GH, our model predicts that IL-6 forms a bridge between the CBDs of IL-6Rα on one side and gp130 on the other. In the model, some exposed residues in the presumptive helices A and C of IL-6 are oriented towards gp130, and might therefore be postulated as required for gp130 binding and activation. Interestingly, we find that mutations in these residues give rise to IL-6 mutants which display the expected properties: (i) reduced biological activity, (ii) unimpaired IL-6Rα binding and (iii) impaired assembly *in vitro* of a receptor complex containing gp130. The same mutants behave as receptor antagonists of wild-type (wt) IL-6 both *in vitro* and in bioassays in human hepatoma cells.

Results

Model of human IL-6 based on the X-ray structure of bovine G-CSF

The growing amount of structural information about hemopoietic cytokines obtained either through X-ray crystallography or NMR has confirmed original predictions based on sequence analysis (Bazan, 1990a) that the antiparallel four-helix bundle motif first observed in porcine GH (Abdel-Meguid *et al.*, 1987) forms the central structural motif conserved in all of these molecules (Diedrichs *et al.*, 1991; De Vos *et al.*, 1992; McKay, 1992; Pandit *et al.*, 1992; Powers *et al.*, 1992; Senda *et al.*, 1992; Hill *et al.*, 1993).

In IL-6 the same general topology has been predicted (Bazan, 1990a, 1991). In a previous study (Savino *et al.*, 1993) we proposed a tertiary structure for human IL-6 (hIL-6) closely related to that observed in GH, where two long loops (the AB loop connecting helices A and B, and the CD loop connecting helices C and D) pack independently against the bundle of four helices. This is in contrast to other cytokines like IL-2, IL-4, GM-CSF and M-CSF where the corresponding loop regions associate intimately to form a short two-stranded antiparallel β-sheet. A parameter that

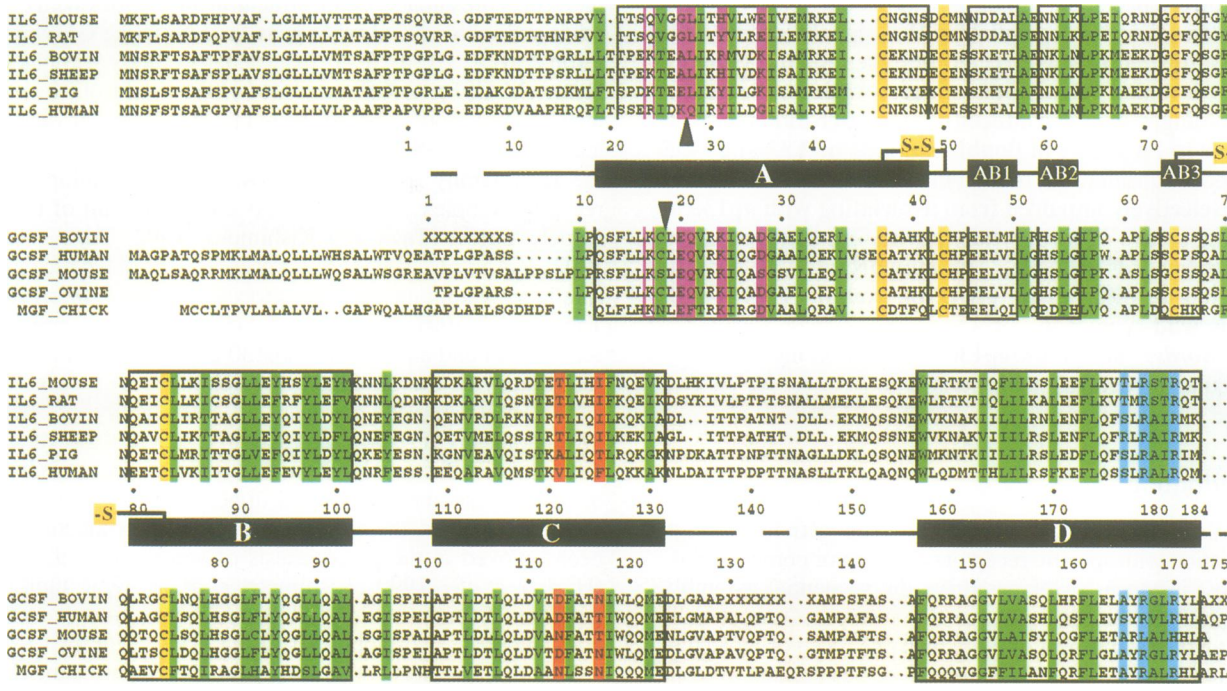

Fig. 1. Multiple sequence alignment between IL-6, G-CSF and MGF. Secondary structure elements of bG-CSF as determined by the DSSP algorithm (Kabsch and Sander, 1983) are indicated by black bars in between the group of aligned IL-6 sequences and the group including G-CSF and chicken MGF. The model of IL-6 predicts that the four helices (A−D) forming the central helix bundle and three short helical segments (AB1, AB2 and AB3) in the AB loop will be conserved. Parts of bG-CSF absent in the X-ray structure are represented by a broken line or by an X in the corresponding sequence (GCSF__BOVIN). N-terminal deletions that retain biological activity of IL-6 (Brakenhoff *et al.*, 1990) or G-CSF (Kuga *et al.*, 1989) are marked by triangles. Sequence numbering is with respect to the mature peptide for IL-6 (IL6__HUMAN) or follows the numbering present in the X-ray structure for G-CSF (GCSF__BOVIN). The conservation of hydrophobic residues that are part of the hydrophobic core of the four-helix bundle or are important for the packing of the AB and CD loops against the bundle, is highlighted in green; the two conserved disulfide bridges are shown in yellow. For L19 and M67 of IL-6 the corresponding functionally similar hydrophobic residues of bG-CSF (L10 and L62) are also shown. On helix D three positions shown to be important for IL-6 binding to the IL-6Rα (site 1) are colored in cyan. Residues of IL-6 at the predicted site 2, the gp130 binding site, which have been mutagenized in this study are colored either magenta (helix A) or red (helix C).

seems to be characteristic for this division into two structural subclasses is the length of the part of the chain involved in forming the four-helix bundle. Shorter molecules like IL-2, IL-4, GM-CSF, M-CSF and IL-5 all adopt the topology first observed in GM-CSF (Diedrichs *et al.*, 1991), whereas longer polypeptides like G-CSF and also IL-6 should resemble more a GH-like fold. The recently determined X-ray structure of G-CSF (Hill *et al.*, 1993) confirms this hypothesis in that, apart from some differences in interhelix packing angles, the overall topology is very similar to that of GH, including the conformation of the AB loop.

Although the pairwise sequence identity between various IL-6 and G-CSF sequences is still low (~20%), a multiple sequence alignment of IL6 and G-CSF (Figure 1) shows that the overall pattern of hydrophobic and hydrophilic amino acids is very well conserved within the α-helical regions. Moreover, both of the G-CSF disulfide bridges constraining the molecule's structure are conserved in all IL-6 sequences, and the few insertions and deletions occur exclusively in loop regions connecting secondary structure elements and can hence be easily accommodated. This suggests an almost precise structural equivalence between G-CSF and IL-6, offering a valid three-dimensional template for homology modeling of hIL-6.

We have therefore used the X-ray structure of bovine G-CSF (bG-CSF) to improve our three-dimensional model of hIL-6 (see Materials and methods). Starting from the sequence alignment given in Figure 1, the bG-CSF residues were replaced with the corresponding amino acids of hIL-6 using the homology modeling option in WHATIF (Vriend, 1990). To optimize the packing of sidechains we first used the sidechain rotamer optimization procedure of WHATIF and subsequently analyzed the result on an interactive graphics workstation using the INSIGHT program (Dayringer *et al.*, 1986). Corrections were applied where necessary taking into account both the conformation of the original amino acid in bG-CSF and the variation of amino acids as predicted from the multiple sequence alignment (Figure 1). Packing of sidechains in the protein interior was further checked by calculation of the solvent accessibility surface. Only two small internal cavities were detected similar in size to the ones also present in bG-CSF. Together with the fact that buried hydrophobic residues were conserved (Figure 1) this proved the compatibility of the one-

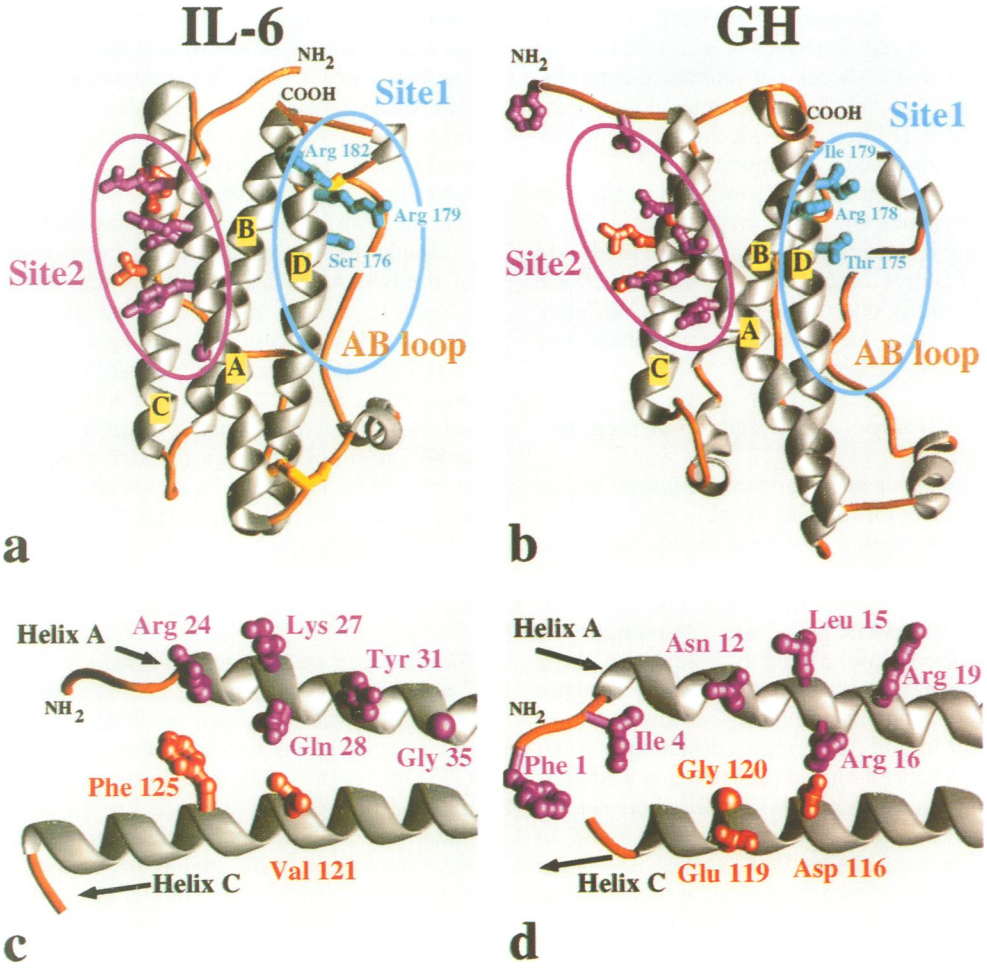

Fig. 2. Superimposition of IL-6 and GH. RIBBONS (Carson, 1987) representation of IL-6 (**a**) and GH (**b**) after superimposing the two molecules (see Materials and methods). In IL-6 and GH the differing orientation of helices A with respect to helices B–D restricts the overlap to the region around site 2. The other three helices including the AB loops show in contrast a rather good correspondence including also site 1 on helix D (blue residues). At sites 2 (opposite sites 1) the corresponding residues of IL-6 and GH are colored magenta (helices A) and red (helices C), respectively. They are shown in more detail for IL-6 (**c**) and GH (**d**). In addition to K27, Q28, Y31 and G35 (helix A) and V121 and F125 (helix C), G35 of IL-6 was also mutagenized to explore a possible extension of site 2 further C-terminally on helix A. For F1 and I4 of GH no corresponding residues exist in IL-6 due to a different conformation of the N-terminal segment preceding helix A. In the case of IL-6 this segment, instead of pointing away from the molecule towards the site 2 receptor, folds over the upper end of the four-helix bundle and closes the hydrophobic core.

dimensional sequence alignment to the three-dimensional context of the template molecule.

More extensive remodeling of the parent bG-CSF structure was only necessary at two places, the short loop connecting helices B and C and the middle of the AB loop (see Materials and methods). These localized changes did not, however, alter the very close overall structural equivalence to the parent bG-CSF and the conservation of secondary structure elements (Figure 1). Only at the N-terminus helix A was shortened by two residues in IL-6 (Figure 1), allowing L19 in the preceding segment to play a role similar to that of L10 in bG-CSF in packing the N-terminal amino acids against the hydrophobic core, like a cap that closes the four-helix bundle (Figures 1 and 2a).

Our model is consistent with all the available mutagenesis data on hIL-6; a tabulation of mutational studies published so far in the framework of the model and a rationalization of the effect of each mutation will be reported elsewhere (A.Lahm, in preparation). The refinement of the IL-6 model led us to reconsider our previous conclusions about a non-helical conformation of the C-terminus based on the observation that IL-6 mutant S176P showed no loss in activity (Savino *et al.*, 1993). Superimposition of the X-ray structure of a mutant lysozyme containing a proline substitution in a helical region (Sauer *et al.*, 1992) on the IL-6 model showed that IL-6 can accommodate a proline mutation at position 176, at the same time retaining the following part of helix D (including sidechains) in a nearly unaltered conformation (data not shown).

In short, apart from minor local differences in the loop regions and the N-terminus, the model predicts that the hIL-6 structure comprising residues 12–184 should preserve most of the structural features of G-CSF, and that functional differences are primarily due to the exposure of different amino acids on the surface, particularly in regions interacting with the corresponding receptors.

Comparison with GH structure: prediction of receptor binding sites

To date the complex between GH and the extracellular part of its homodimeric receptor remains the only system where interaction surfaces between a four-helix bundle factor and CBD carrying receptors have been unambiguously identified on a structural basis (De Vos *et al.*, 1992). The ligand has two sites, located on opposite sides, site 1 (binding to the first receptor to form a low affinity complex) and site 2 (binding to the second receptor and triggering receptor dimerization). Site 1, encompassing the C-terminal part of helix D and portions of the AB loop, is considerably wider than site 2, which is located on helix A including also parts of helix C. The significant sequence similarity between the extracellular domains of the GH receptor and those of IL-6Rα and gp130 (Bazan, 1990a, 1990b) as well as a similar sequential assembly of two receptor components leading to a ternary homo- or heterodimeric receptor complex, respectively (Taga *et al.*, 1989; Cunningham *et al.*, 1991), suggest that the scaffold of tertiary interactions seen in receptor complex assembly by GH might also be reproduced for IL-6. Therefore, also IL-6 should have a site 1 required for IL-6Rα binding and a site 2 for interaction with gp130. The idea of two functionally distinct regions in IL-6 has been previously suggested by mutagenesis studies and epitope mapping with neutralizing monoclonal antibodies (Brakenhoff *et al.*, 1990, 1992). Furthermore, the identification of hIL-6 R179 as the major receptor binding determinant on hIL-6 helix D (Leebeeck *et al.*, 1992; Fontaine *et al.*, 1993; Savino *et al.*, 1993) suggests its functional and structural equivalence to GH helix D residues T175 or R178 at the center of site 1 (De Vos *et al.*, 1992; see also Figure 2a and b). We reasoned therefore that it could be possible to use our IL-6 model in order to predict, with a certain degree of accuracy, the composition of site 2 and confirm the model by site-directed mutagenesis.

The model of hIL-6 was superimposed onto GH in the context of the complex with the GH receptor (De Vos *et al.*, 1992). Due to slightly different helix packing angles it was not possible to superimpose helices A and D of both molecules simultaneously on a residue by residue basis (see Materials and methods). Instead, we chose an intermediate solution (Figure 2, upper part) where only parts of helices A, B and C were used in calculating the superimposition (see Materials and methods). Except for helix A, the resulting structural overlap is generally good, bringing IL-6 and GH residues at sites 1 on helix D close to each other. For helices A significant overlap occurs only around site 2 (Figure 2a and b). Interestingly, also the AB loops show qualitatively good spatial overlap, which suggests that this region is also important for the recognition of hIL-6Rα, as found for the corresponding region of GH (Cunningham and Wells, 1990; De Vos *et al.*, 1992). This is supported by the observation that when residues of hIL-6 constituting the presumptive AB loop are replaced with the corresponding mIL-6 residues (mIL-6 does not bind to hIL-6Rα) the chimeric molecule is totally unable to bind to hIL-6Rα, while it maintains proper folding (Fiorillo *et al.*, 1992a; van Dam *et al.*, 1993).

Despite the overall difference in the relative orientation of the two A helices, the match around site 2 was good enough to identify six residues on hIL-6 helices A and C as being close to residues forming site 2 in GH (indicated in red and purple in Figure 2): R24, K27, Q28 and Y31 on helix A, and V121 and F125 on helix C. Of these, R24 was not mutagenized since N-terminal deletions of hIL-6 up to K27 result in a biologically active molecule (Brakenhoff *et al.*, 1989). G35 on helix A was also mutagenized in order to map a possible further extension of the gp130 binding site on helix A. On helix C, V121 and F125 were mutated, assuming that F125 of IL-6 was equivalent to the neighboring E119 and G120 of GH (Figure 2c and d).

Site-directed mutagenesis of helices A and C

The hIL-6 residues identified as candidates in making contact with gp130 were mutated by PCR at the cDNA level as described in Materials and methods. With the exception of G35, all residues indicated in the previous heading were mutated into alanine, which is known not to disturb helix conformation. For some residues more dramatic changes were introduced in the attempt to generate steric or charge repulsions. Therefore, G35 of hIL-6 was replaced with bulky residues like leucine, glutamine, arginine, histidine and phenylalanine. In place of Y31 and F125, which are already large and hydrophobic, we introduced serine and valine, respectively (as well as alanine) to change the size once again, and also aspartic acid in both positions to change both size and hydrophobicity. Finally, in addition to aspartic acid and alanine, V121 was also changed into larger residues such as phenylalanine or tyrosine, again with the hope that steric hindrance would result. For all mutations we tried to avoid substitutions that would restore the murine IL-6 (mIL-6)

sequence at the corresponding position, keeping in mind that mIL-6 in complex with mIL-6Rα is active on human cells (Fiorillo *et al.*, 1992b). To analyze biological activity, we selected a total of 27 mutants, two of which, unexpectedly, carried additional substitutions, either at position 36 (I36T) or 42 (E42A), where we had not introduced degenerate codons in the oligonucleotides used for the mutagenic PCR. Wild-type and mutant hIL-6 molecules were produced in the *Escherichia coli* periplasmic space as described in Materials and methods.

Biological activity and receptor binding of mutants in the predicted helix A

The biological activity of helix A mutants was tested on human hepatoma Hep3B cells, where IL-6 is able to enhance transcription from a transfected human C-reactive protein promoter fused to the reporter CAT gene (Fiorillo *et al.*, 1992a; Fontaine *et al.*, 1993; Savino *et al.*, 1993). We have recently improved this assay using as reporter the gene coding for a secreted form of alkaline phosphatase (SEAP) (Gregory *et al.*, 1994). The secreted enzyme is easily assayed in the supernatant of transfected cells by measuring the conversion of a phosphatase substrate, a reaction which increases the absorbance at 405 nm (see Materials and methods).

The biological activities of IL-6 mutants in the predicted helix A are shown in Table I. A first observation is that none of the single point mutations dramatically reduces biological activity, but a significant effect is seen with mutant Y31D (2.5-fold reduction).

A different pattern is obtained, however, with double mutants. Double substitutions involving K27 and G35 retain levels of bioactivity comparable to that of wt IL-6, in line with previous observations obtained with hIL-6 deletions (Brakenhoff *et al.*, 1989). Also, double mutations Q28A/Y31A and Q28A/Y31S do not seem to affect bioactivity significantly. However, when the mutation Y31D is combined with either Q28A or with a bulky hydrophobic residue in position 35 (Y, F or L) the decrease of activity is more dramatic than just the combination of the single mutations (Table I), with a reduction ranging from 15-fold (Q28A/Y31D) to 50-fold (Y31D/G35F). The weak activity elicited by these mutants is characterized by a maximal response lower than that of wt IL-6, which is characteristic behavior of partial agonists. As an example, the dose–response curves of wt IL-6 and of IL-6 Y31D/G35F in a typical experiment are shown in Figure 3. Finally, when mutation Y31D is combined with a small (G35C) or hydrophilic (G35H) amino acid in position 35, the effect is very similar to that caused by the Y31D mutation alone.

The reduction of biological activity observed for some mutants could be due either to them being impaired from recruiting gp130 in a functional multiprotein receptor complex (as the model predicts) or to loss of binding to IL-6Rα if the residues are part of the binding surface of the specific receptor (site 1) or if the mutations cause partial or total misfolding of the cytokine. In order to discriminate between these possibilities, *in vitro* solid phase binding assays to a soluble form of IL-6Rα were systematically carried out for all mutants which showed biological activity reduced by a factor of two or more. One single and one double mutant which showed wt levels of biological activity were also tested for receptor binding as positive controls. The results are summarized in Table I. With the exception of the double mutation Q28A/Y31D, no single, double or triple substitutions significantly reduced binding to soluble hIL-6R (shIL-6Rα), regardless of the level of residual biological activity on Hep3B hepatoma cells (Table I). This was consistent with the prediction that receptor binding would not be altered because the mutated residues should lie on

Table I. Biological activity and receptor binding of predicted helix A mutants

Predicted helix A mutations	Biological activity (%)[a]	Receptor binding (%)[a]
K27A	74 ± 24%	100 ± 1%
Q28A	100 ± 18%	NT
Y31D	**39** ± 3%	111 ± 19%
G35R	100 ± 3%	NT
G35F	95 ± 28%	NT
G35L	76 ± 2%	NT
G35C	100 ± 1%	NT
K27A G35R	125 ± 25%	NT
K27A G35Q (I36T)	80 ± 19%	100 ± 4%
Q28A Y31A	75 ± 15%	NT
Q28A Y31S	100 ± 21%	NT
Q28A Y31D	**8.5** ± 3%	**19** ± 1%
Y31D G35Y	**4.5** ± 1%	73 ± 17%
Y31D G35F	**2** ± 0.8%	84 ± 9%
Y31D G35L (E42A)	**5.2** ± 4%	188 ± 16%
Y31D G35H	**38** ± 8%	85 ± 15%
Y31D G35C	**30** ± 1%	82 ± 18%

[a]Relative to wt.
Activities reduced by a factor of two or more (relative to wt activity) are shown in bold.
NT, not tested.

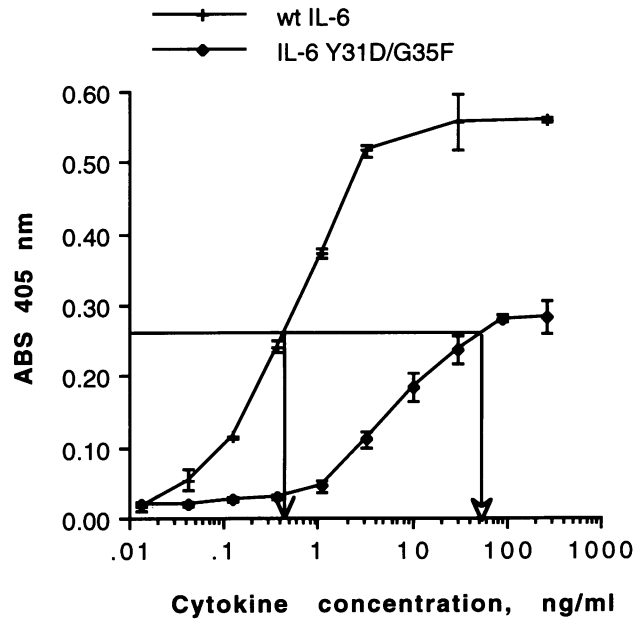

Fig. 3. Dose–response curves for wt IL-6 and for IL-6 Y31D/G35F. The activity of the secreted alkaline phosphatase (SEAP) reporter gene is assayed by measuring the conversion of a phosphatase substrate which increases the absorbance at 405 nm (Gregory *et al.*, 1994). The biological activity of IL-6 Y31D/G35F is calculated (as described in Materials and methods) as the ratio between the concentration of wt IL-6 and the concentration of mutant IL-6 necessary to give half-maximal stimulation (calculated as 0.27 OD_{405} units and indicated by a horizontal line) and was ~1.2% in this particular experiment.

Table II. Biological activity and receptor binding of predicted helix C mutants

Predicted helix C mutations	Biological activity (%)[a]	Receptor binding (%)[a]
V121Y	125 ± 53%	NT
V121D	58 ± 23%	78 ± 2%
F125V	153 ± 14%	102 ± 2%
V121F F125V	159 ± 1%	NT
V121Y F125V	225 ± 52%	80 ± 4%
V121D F125V	171 ± 19%	94 ± 5%
V121Y F125Y	103 ± 3%	NT
V121Y F125D	141 ± 22%	NT
V121D F125D	104 ± 6%	NT
V121A F125A	100 ± 2%	NT

[a]Relative to wt.
NT, not tested.

the cytokine surface opposite that binding to IL-6Rα. On the other hand, the parallel decrease of bioactivity and receptor binding of mutant Q28A/Y31D might indicate that this mutation induces a partial misfolding of the molecule. Finally, we unexpectedly found that the triple mutant IL-6 Y31D/G35L/E42A has a slight but very reproducible increase in receptor binding (188 ± 16%, average and standard deviation of four independent binding experiments on three independent protein preparations and quantifications).

Biological activity and receptor binding of mutants in the predicted helix C

The mutants in the predicted helix C were subjected to the same kind of analysis; the results are shown in Table II. As for the mutations on helix A, no single mutation significantly reduced biological activity. However, unlike the previous case, the combination of various substitutions of V121 and of F125 never reduced biological activity. Instead, when a valine replaced F125, either as a single mutation or in combination with other mutations at position 121, the corresponding mutant showed a moderate increase of activity (Table II).

Mutants which showed bioactivity altered by a factor of two or more were tested for *in vitro* receptor binding; the results are shown in Table II. No single or double mutations tested altered binding to shIL-6Rα, further substantiating the hypothesis that the mutated region is not functionally or structurally involved in binding the IL-6Rα. Consequently, the moderate increase in bioactivity seen for all the F125V mutants would not appear to be the result of an increased receptor affinity, but might be due to minor rearrangements around site 2.

Mutant IL-6 Y31D/G35F fails to promote the association between soluble IL-6R and soluble gp130 in vitro

The three IL-6 variants (IL-6 Y31D/G35Y, IL-6 Y31D/G35F and IL-6 Y31D/G35L/E42A) that maintained unaltered or even improved receptor binding but showed severely reduced levels of biological activity (Table I) are likely to be defective in binding to gp130 as predicted by molecular modeling (see above).

It has already been shown (Yasukawa *et al.*, 1992; Mullberg *et al.*, 1993; Sporeno *et al.*, 1994) that non-

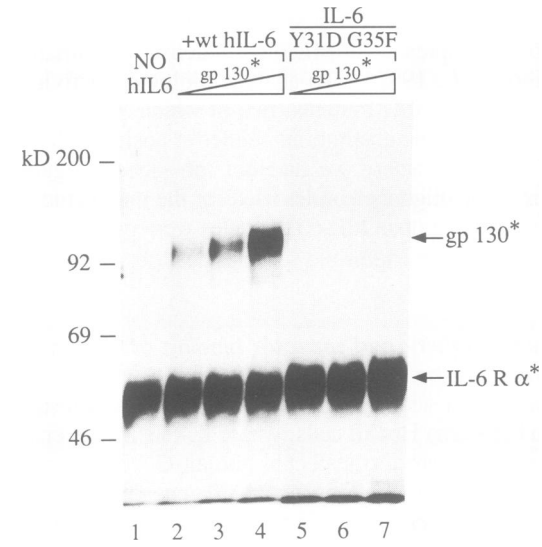

Fig. 4. IL-6 Y31D/G35F fails to immunoprecipitate soluble hgp130. Approximately 1 μg of shIL-6Rα (see Materials and methods) was immunoprecipitated (using the anti-IL6-Rα monoclonal antibody I6R1/9) in the presence of 5 μg of wt hIL-6 (lanes 2–4), in the presence of 5 μg of IL-6 Y31D/G35F (lanes 5–7) or without hIL-6 (lane 1). A total of 100 μl (lanes 2 and 5), 200 μl (lanes 3 and 6) or 500 μl (lanes 1, 4 and 7) of labeled sgp130 (see Materials and methods) were also added to the immunoprecipitation reactions.

neutralizing monoclonal antibodies against shIL-6Rα are able to co-immunoprecipitate recombinant shIL-6Rα and recombinant soluble human gp130 (sgp130) only in the presence of hIL-6. We therefore investigated whether one of the three mutants listed above was still able to promote coimmunoprecipitation of sgp130 and shIL-6Rα. For this experiment we chose the mutant with the lowest residual bioactivity, IL-6 Y31D/G35F (see Table I). As shown in Figure 4, in the presence of 5 μg of wt hIL-6, there is a good correlation between the amount of labeled sgp130 added in the immunoprecipitation reaction and the amount of sgp130 present in the immunoprecipitate (Figure 4, lanes 2–4), whereas in the absence of IL-6 no sgp130 is present in the pellet (Figure 4, lane 1). In the presence of the same amount of Y31D/G35F no sgp130 was found in the immunoprecipitate (Figure 4, lanes 5–7).

We then asked whether mutant IL-6 Y31D/G35F was able to compete for the binding of wt IL-6 to IL-6Rα in the same immunoprecipitation assay and therefore to inhibit the recruitment of sgp130 by wt hIL-6. In pilot experiments we determined 100 ng as the minimal amount of hIL-6 needed to obtain a strong (but not saturated) signal of labeled sgp130 in the pellet when adding 500 μl of labeled sgp130 (see Materials and methods) to the immunoprecipitation reaction (data not shown). We then performed similar experiments in the presence of fixed amounts of both sgp130 (500 μl, labeled *in vivo*) and wt hIL-6 (100 ng) and increasing amounts of IL-6 Y31D/G35F. The result is shown in Figure 5. The amount of sgp130 immunoprecipitated by wt IL-6 is reduced by a 10-fold molar excess of the competitor (Figure 5, lane 6) and is almost completely abolished at a 100-fold molar excess (Figure 5, lanes 7 and 8). Therefore, mutant IL-6 Y31D/G35F acts as an antagonist of wt IL-6 in the assembly of a complex with shIL-6Rα and sgp130 *in vitro*. Similar results were obtained using mutant IL-6 Y31D/G35L/E42A (data not shown).

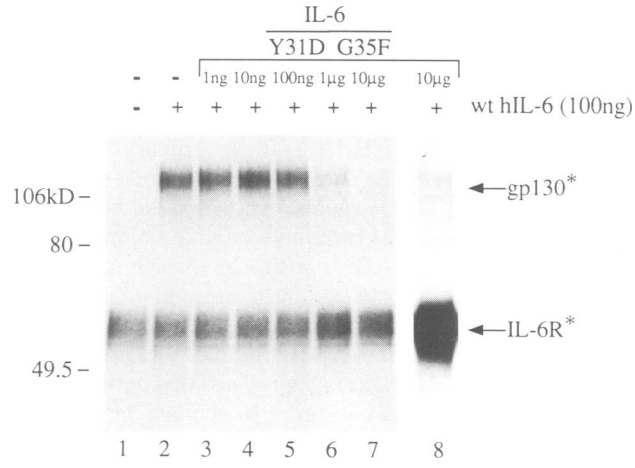

Fig. 5. IL-6 Y31D/G35F acts as a receptor antagonist of hIL-6 *in vitro*. Approximately 1 µg of soluble hIL-6Rα and 500 µl of sgp130 (see Materials and methods) were immunoprecipitated with the anti-IL-6Rα monoclonal antibody I6R1/9 in the absence (lane 1) or presence (lanes 2–8) of 100 ng of wt hIL-6. Various amounts (indicated above the lanes) of mutant IL-6 Y31D/G35F were added to the immunoprecipitation reaction. Lanes 1–7: 16 h exposure; lane 8: same gel track as lane 7 after 120 h exposure.

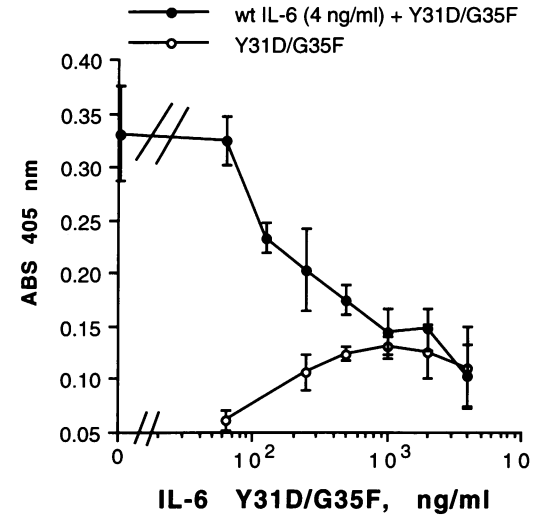

Fig. 6. IL-6 Y31D/G35F acts as a partial receptor antagonist of hIL-6 *in vivo*. Human Hep3B cells were incubated with increasing amounts of IL-6 Y31D/G35F in the presence (wt IL-6+Y31D/G35F) or in the absence (Y31D/G35F) of 4 ng/ml of wt IL-6. The SEAP reporter gene activity was assayed as in Figure 3.

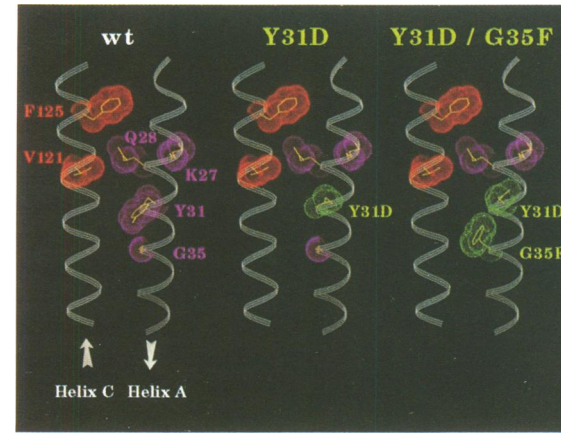

Fig. 7. Single Y31D and double Y31D/G35F mutation on helix A. Residues at IL-6 site 2 on helix A (magenta) and C (red) are shown together with the sidechain's van der Waals surface. Mutated residues are colored green. In contrast to the single mutation Y35D (middle), where the aspartate sidechain can move independently of position 35, the presence of F35 in the double mutant (right) might force D31 in a position resulting with higher efficiency for blocking the interactions with gp130. Alternatively, steric hindrance by F35 could make it more difficult for gp130 to escape the effect of the D31 mutation through subtle changes of its conformation in the interface.

Antagonism of wt IL-6 action by IL-6 Y31D/G35F on Hep3B cells

The extent to which IL-6 Y31D/G35F was able to act as an antagonist of wt IL-6 activity on cultured cells was then determined *in vivo*. Human Hep3B hepatoma cells were incubated with increasing amounts of IL-6 Y31D/G35F in the presence or absence of 4 ng/ml of wt IL-6 and the biological response of cells was quantified as described in Materials and methods. The results are shown in Figure 6. Mutant IL-6 Y31D/G35F inhibits 50% of wt IL-6 biological activity at a concentration of 500 ng/ml, corresponding roughly to a 100-fold molar excess of competitor. The biological activity of cells induced with the cocktail of mutant and wt IL-6 could not be distinguished from that observed in the mutant alone at a concentration of 4 µg/ml. The drop in biological activity illustrated in Figure 6 could be fully reversed by adding a large excess (100 ng/ml) of wt hIL-6 (data not shown), thus demonstrating that a large dosage of Y31D/G35F is not toxic. The antagonistic action of IL-6 Y31D/G35F on Hep3B cells argues against the possibility that the reduced biological activity of the mutant might be due to its instability at 37°C (the mutant is known to be properly folded at 25°C because it binds the soluble IL-6Rα *in vitro*: see Materials and methods) and instead suggests that it remains stable in culture medium at 37°C for the 65 h of duration of the biological assay.

Discussion

In the first part of this work we describe a refinement of our previous three-dimensional model of hIL-6 which takes into account the recently published X-ray structure of the related cytokine, G-CSF (Hill *et al.*, 1993). The model predicts that these two structures are almost completely superimposable with each other and with GH, and this includes the conformation of the AB loop.

The close resemblance between the GH structure and our IL-6 three-dimensional model has received functional support from recent mutagenesis studies on the C-terminus, which have demonstrated at least a partial overlap between site 1 in GH and the binding site for IL-6Rα in IL-6, which by analogy we also call site 1. We have thus assumed that the same general topology might be adopted by both GH and IL-6 in forming a ternary receptor complex. This implies that the binding of gp130 after IL-6 has interacted with IL-6Rα is not primarily or exclusively due to a postulated change in IL-6Rα conformation (Hirano *et al.*, 1990), but rather to the cooperative interaction between gp130 binding surfaces present both on IL-6 and IL-6Rα. In this way the IL-6 molecule, like GH, operates as a bridging ligand enabling IL-6Rα and gp130 to associate and form the ternary high affinity complex, despite their intrinsic lack of affinity for each other. The superimposition of IL-6 onto GH led

us to postulate that, if sites 2 overlap as sites 1 do, the corresponding residues in IL-6 (namely 24, 27 or 28, 31 and 35 in helix A, and 121 and 125 in helix C) would form the gp130 binding site, and that with a reasonable expectation mutations in these residues would lead to selective loss of signal transduction.

We were nonetheless aware of relevant issues raised from previous studies on GH. Through alanine scanning mutagenesis of the N-terminal region, Cunningham *et al.* (1991) identified only I4 as essential for binding to the second receptor, whereas residues N12, R16, R19, D116 and E119, which form the actual binding site as revealed by the X-ray structure of the complex (De Vos *et al.*, 1992), showed a much less pronounced effect. Similarly, residue R24 in IL-6, postulated by the model as being part of site 2, can be deleted without loss of activity (Brakenhoff *et al.*, 1989). This result, on the other hand, might also testify to substantial differences between GH and IL-6 in the distribution of site 2 residues. In order to gain better insights into this issue we extensively mutagenized all the other site 2 residues predicted for both helices.

The results point to the existence of both differences and analogies between the two receptor systems. One important difference is the fact that V121 and F125 in helix C are of minor importance, since neither single nor double mutations produced a significant drop in bioactivity. This is somewhat surprising since the corresponding region of GH has not only been identified as part of the GH receptor interface, but also as containing the G120R mutation, which acts as a powerful antagonist (Fuh *et al.*, 1992). This finding implies that the mode of interaction in the IL-6 system is not identical to that observed in the GH system.

On the other hand, the validity of our model was confirmed by the fact that a subset of helix A mutants involving specific substitutions of Y31 and G35 showed the expected phenotype. The behavior of single and double substitutions indicates that Y31 is more important than G35. Indeed, the only single mutant showing a detectable and reproducible decrease of activity was Y31D, whilst none of the substitutions of G35 with different amino acids resulted in significantly altered activity. However, since a further substantial drop was achieved by combining Y31D with mutations at G35, one has to assume that the latter is located at the edge of the interaction surface. A possible explanation for the results observed for some of these double mutations (Table I) might be found in the stereochemical constraints imposed on these amino acids on the surface of helix A (Figure 7). Although the introduction of the negative charge of D31 apparently reduces the interaction with gp130, only the presence of a big hydrophobic residue at the neighboring position 35 could lock it into a conformation incompatible with efficient gp130 binding, whereas smaller residues like Cys or more hydrophilic substitutions like His would not exert the same effect, thus resulting in an essentially unchanged phenotype (Table I).

Our finding, that in IL-6 only one subset of mutation's residues 31 and 35 are biologically impaired, emphasizes an important difference between sites 1 and 2 which is parallel to that observed in GH. Site 1, which is responsible for the formation of an initial low affinity complex, has to be very specific and therefore does not tolerate modifications of key residues (Savino *et al.*, 1993). Site 2 (which has no intrinsic affinity for the second receptor and is only functional in combination with the dimerization of receptor molecules), instead, might be expected to tolerate better non-conservative substitutions as gp130 is common to, and therefore has to interact with all the members of the IL-6 family, that show no or only limited similarity in their primary sequence (Kishimoto *et al.*, 1992; Taga and Kishimoto, 1992; Yin *et al.*, 1993). This observation suggests that the interaction surface of gp130 must be extremely flexible, in order to be able to contact five surfaces not similar to each other. We have indeed found that we can introduce non-conservative substitutions in all the positions mutagenized (for example K27A, Q28A, Q28A/Y31A, G35R and V121D/F125D) without decreasing biological activity, and that quite specific substitutions are required in order to achieve antagonistic effects. We have so far introduced only a subset of possible substituents and we cannot thus exclude that more dramatic consequences would be obtained by utilizing other amino acid combinations.

Our *in vitro* data suggest that specific Y31/G35 mutations cause a failure to trigger efficient association with gp130. It should be kept in mind, however, that the sensitivity of our immunoprecipitation assay is limited by the amount of labeled sgp130 added to the reaction. Therefore, even if we cannot detect any gp130 in the immunoprecipitate in the presence of the mutant IL-6 Y31D/G35F (Figure 4), it is not possible to rule out the possibility that some weak interaction ($<3\%$ of the wt) is still taking place, which would be below the detection level of our assay. This could easily account for the residual activity of the mutant at very high concentrations (Figure 3). This fact might raise problems for the development of a full IL-6 antagonist, which would require a total loss of binding to gp130. Alternatively it may constitute an advantage if, for therapeutical purposes, a partial antagonist is more desirable in order not to inhibit other important physiological activities of the cytokine.

The *in vitro* competition assays also indicate that the IL-6 Y31D/G35F mutant is able to displace wt IL-6 from the 'ternary' complex only at a 100-fold molar excess. This was somewhat expected since wt IL-6, which binds both receptors, is known to form high affinity complexes ($K_d \approx 10^{-11}$) (Hibi *et al.*, 1990), whereas the antagonist, which can interact efficiently only with one receptor, namely IL-6Rα, should have a much lower affinity corresponding to the formation of a low-affinity complex ($K_d \approx 10^{-9}$). It will be interesting to test this idea by Scatchard analysis of the interaction of wt and mutant proteins on the cell surface. This finding has practical implications for the possible use of IL-6 antagonists in therapy, because high doses of this molecule would be required unless other mutations are introduced in order to improve site 1 affinity for IL-6Rα.

While this work was in progress, it was shown that dimerization of the signal transducer gp130 takes place on the surface of cells after stimulation with IL-6 and is absolutely necessary for signaling (Murakami *et al.*, 1993). One way to envisage gp130 dimerization could be that when two ternary complexes of the type postulated in this study form they are led to associate with each other by still unknown mechanisms. Alternatively, gp130 dimerization might be due to the simultaneous binding of two gp130 molecules to different subsites of a single IL-6 molecule. This last idea requires that at least three receptor molecules are present in a functional complex and implies that the mode

of association of the single components into the complex is related to, but nevertheless distinctly different from, that observed for GH. Looking at the particular association of GH with its receptors one can, however, imagine that changes in the relative orientation (translations, rotations) of all or some of the components involved would be possible without destroying the basic feature of the system: a cytokine (or hormone) which bridges receptor molecules that have no intrinsic affinity for each other. If this is the case, the complex of IL-6, IL-6Rα and gp130 might represent a variation on the GH theme that allows the incorporation of a third receptor molecule, namely a second gp130. This would imply that IL-6 site 2 is composed of two subsites. Since our mutagenesis data and the results from the modeling of IL-6 suggest both similarities to and differences from the GH system, neither of these two alternatives can be excluded. Whichever of these models turns out to be true, the fact that helix A is involved in the association with gp130 strongly suggests that IL-6, in the same ways as GH, serves as a bridging ligand that triggers the assembly of the ternary complex. Deciphering more complex interactions in the IL-6 system will require additional experiments and, in particular, data that clearly define the stoichiometry of *in vitro* binding studies.

In conclusion we have here demonstrated that molecular modeling studies and predictions of IL-6R assembly have been applied successfully to better understanding multi-subunit receptor assembly and to furthering our knowledge of the mechanisms required to generate tools for an anti-cytokine therapeutic strategy.

Materials and methods

Model building

Sequences of IL-6, G-CSF (except for bG-CSF) and chicken myelomonocytic growth factor (MGF) included in the multiple alignment (Figure 1) were extracted either from release 25.0 of the SwissProt protein sequence databank (entries IL6_HUMAN, IL6_MOUSE, IL6_RAT, IL6_SHEEP, IL6_PIG, IL6_BOVIN, CSF3_HUMAN, CSF3_MOUSE, MGF_CHICK), from release 37.0 of the EMBL nucleotide database (GCSF_SHEEP; translated from entry OOCSFGR) or in the case of GCSF_BOVIN from the coordinate file of the 1.7 Å bG-CSF X-ray structure provided by B.Lovejoy, D.Cascio and D.Eisenberg (protein databank pre-release entry 1BGC). In the GCSF_BOVIN sequence residues not visible in the electron density map have been given the symbol X. The sequences were aligned using the PILEUP program of the GCG sequence analysis package (Devereux *et al.*, 1984) and some minor corrections were applied manually. As a template for modeling the structure of bG-CSF was used instead of the canine G-CSF (pre-release entry 1BGD) since it was solved at higher resolution and was more complete.

The model of hIL-6 was initially constructed using the homology modeling option of the molecular modeling program WHATIF (Vriend, 1990) including optimization of sidechain rotamer conformations. Corrections to optimize packing of sidechains in the hydrophobic core were manually applied on an interactive graphics workstation using the program INSIGHT (Dayringer *et al.*, 1986) assessing remaining internal cavities through calculation of solvent accessibility surfaces (probe radius 1.8 Å) with the PQMS program (Connolly, 1993). The few deletions or insertions of hIL-6 with respect to bG-CSF in the loop regions, as well as the part preceding the first helix A, were modeled manually using various tools of the INSIGHT program. The region of the AB loop in IL-6 from P65 up to G72 had to be remodeled due to an insertion present in this segment. M67 of IL-6 was assumed to take the role of bG-CSF L62, that packs the AB loop against the rest of the structure. This fits well with chemical modification studies identifying IL-6 M67 as the methionine most resistant to oxidation (Nishimura *et al.*, 1991). In the short loop connecting helices B and C, the F105 of IL-6 was put into a position similar to I96 of bG-CSF to maintain the contribution of this loop to the hydrophobic core. The least reliable part of the IL-6 model is the region of the CD loop (only partially present in the bG-CSF structure) where positions 131–156 were modeled tentatively placing hydrophobic residues towards the four-helix bundle. After the remodeling, energy minimization was applied to release some of the strain introduced during the manual manipulations. The resulting mainchain conformation of the IL-6 model falls within the allowed region of the Ramachandran plot excluding G72 in the AB loop and positions where the parent bG-CSF structure already had an unusual mainchain conformation. To evaluate the effect of a proline substitution at S176 on IL-6 helix D, residues 66–71 of the X-ray structure of a D72P lysozyme mutant that have a substitution within a helical region (PDB entry 1L76; Sauer *et al.*, 1992) were superimposed onto residues 170–175 of the IL-6 model.

Superimposition of IL-6 and GH

For comparison with the structure of the GH receptor complex stucture, the complete structure was generated from the C-α coordinates present in the protein databank pre-release entry 2HHR (Bernstein *et al.*, 1977) using WHATIF. After sidechain rotamer optimization, the GH receptor complex structure was manually inspected and corrected according to the published details (De Vos *et al.*, 1992). To identify residues in IL-6 and GH that are in structurally equivalent positions, we initially superimposed the molecules including only subsets of residues from either helix A or D. This gave, however, no satisfactory superimposition for either site 1 (helix D and AB loop) or site 2 (beginning of helix A and end of helix C) since rather than packing nearly parallel like IL-6, helix A and D of GH show a higher crossover angle induced by the short helical segment between helices B and C absent in the IL-6 model (Figure 2). We therefore decided upon a different strategy and superimposed the two molecules, manually placing IL-6 residues R179 and R182 on helix D close to T175, R178 and I179 of GH, i.e. superimposing approximately sites 1 on helices D. The overlap for the other three helices A, B and C was then manually optimized, trying at the same time to achieve an acceptable structural correspondence at site 2. Residues of the two molecules thus identified as being spatially close were subsequently used to calculate the superimposition shown in Figure 2, giving an r.m.s. deviation of 1.82 Å for 52 C-α coordinates (residues 9–27, 72–84 and 107–126 of GH and residues 21–39, 80–92 and 112–131 of IL-6).

Generation of substitution mutants

All mutants were constructed using plasmid pHenΔhIL-6, a derivative of pHEN1 (Hoogenboom *et al.*, 1991). In pHenΔhIL-6 the coding region for hIL-6 is cloned in-frame downstream of the PelB secretion leader and upstream of the C-terminal part (codons 250–406) of the M13 bacteriophage pIII protein; the entire transcription unit is under the control of the *lacZ* promoter. The coding regions of hIL-6 and pIII are separated by an amber AUG stop codon; in *SupE*$^-$ bacterial strains only the PelB–hIL-6 fusion protein will be translated and directed into the periplasmic space. In the hIL-6 coding regions a *Sac*I site spanning codons 20–22, a *Bfr*I site spanning codons 38–40 and a *Bgl*II site spanning codons 168–169 were introduced without changing the encoded sequence; all three sites are unique in the plasmid, like the natural *Xba*I site spanning codons 131–134 of mature hIL-6.

All mutants were constructed by PCR. Amplified fragments were cut with *Sac*I and *Xba*I and ligated into the recipient pHenΔhIL-6 cut with the same enzymes. The identity of all mutants was verified by sequence analysis (Sanger *et al.*, 1977) over the entire PCR amplified region.

Some of the mutant cDNAs were also subcloned into *E.coli* expression vector pT7.7 (Studier and Moffatt, 1986).

Expression of mutant proteins

Human IL-6 mutant proteins were produced in two alternative systems: *Production of secreted forms of hIL-6 in E.coli periplasmic space*. Plasmids derived from pHenΔhIL-6 were transferred into *E.coli* BL 21 (DE3) *LysE* strain (*SupE*$^-$ genotype). A single colony was used to inoculate 2 ml of Luria broth containing 100 μg/ml ampicillin and 1% glucose and grown overnight with shaking at 25°C. A total of 0.5 ml of the saturated culture was diluted 1:100 in Luria broth containing 100 μg/ml ampicillin and 0.1% glucose, and grown in shaken flasks at 25°C. When absorbance at 600 nm reached 0.6, the culture was spun, washed once with 50 mM NaCl and resuspended in 50 ml of Luria broth containing 100 μg/ml ampicillin and 0.4 mM isopropyl thiogalactopyranoside (IPTG). Growth was continued in shaken flasks for 3 h at 25°C. After induction, cells were collected by centrifugation and resuspended in 1.25 ml of 20% sucrose, 30 mM Tris–HCl pH 8, 1 mM EDTA pH 8. A total of 140 μl of the same solution containing 10 mg/ml of freshly dissolved lysozyme was then added following 10 min incubation in ice. After spinning at top speed in a bench-top centrifuge for 10 min at 4°C, supernatants (containing the periplasmic fraction) were recovered and filtered through 0.22 μm low protein binding Millipore filters. *Production in inclusion bodies*. Plasmids derived from pT7.7 (containing hIL-6 cDNA with selected mutations) were also transferred into *E.coli* BL21

(DE3) LysE strain which expresses the T7 RNA polymerase under the inducible *lacUV5* promoter (Studier *et al.*, 1990) and recombinant proteins were produced in large amounts according to Arcone *et al.* (1991).

Quantification of mutant proteins

Mutant proteins expressed as secreted polypeptides in the periplasmic space as described above were quantified as follows: a total of 20 μl of each preparation was analyzed by 0.1% SDS–15% PAGE and stained with Coomassie brilliant blue R-250. The amount of IL-6 mutant protein in each preparation was determined by densitometric scanning of the SDS–polyacrylamide gels and normalization to known amounts of wt recombinant hIL-6 [purified to homogeneity according to Arcone *et al.* (1991)] loaded on the same gel as standards. Densitometric analysis was performed using the Image 1.22y software (NIH, Bethesda, MD).

Bioassays

Bioassays on human Hep3B hepatoma cell line were performed as described (Gregory *et al.*, 1994). Cells were induced in triplicate with serial dilutions of wt and mutant hIL-6 molecules and the conversion of the substrate for the secreted alkaline phosphatase (SEAP) reporter gene was quantified by recording the A_{405} of the cell culture supernatants (Gregory *et al.*, 1994). Dose–response curves were determined in each case and the biological activity of each mutant (expressed as percentage of wt activity) was determined as the ratio between the concentration of wt IL-6 and the concentration of mutant IL-6 necessary to give half-maximal stimulation.

In vitro binding assays

In vitro binding assays between hIL-6 and hIL-6Rα were performed essentially as described by Honda *et al.* (1992). The materials used were (i) recombinant hIL-6 produced in *E.coli* (Arcone *et al.*, 1991), (ii) recombinant shIL-6Rα purified from the culture supernatant of a CHO cell stable transformant clone (CsRh14) generated according to Yasukawa *et al.* (1990), which constitutively secretes the extracytoplasmic region of hIL-6Rα into the medium and (iii) the anti-hIL-6Rα monoclonal antibody I6R 1/9 partially purified from the medium of the established hybridoma cell line by ammonium sulfate precipitation. Details of its production and purification will be published elsewhere (Sporeno *et al.*, 1994). Polystyrene 96-well microplates (Nunc-Immunoplate MaxisorP) were coated with recombinant hIL-6 by adding to each well 100 μl of a 10 μg/ml recombinant hIL-6 solution in 100 mM Tris–HCl, pH 8.0, followed by blocking with TBS-T (TBS + 0.05% Tween 20). After washing, 10 ng of recombinant shIL-6Rα were added to each well and the reaction was incubated for 3 h at 25°C. Bound receptor was detected by sequential incubation with mouse anti-hIL-6Rα monoclonal antibody I6R1/9 (1:3000 dilution in TBS-T, 100 μl/well) and AP-conjugated goat anti-mouse IgG (1:5000 dilution in TBS-T, 100 μl/well) and *p*-nitrophenyl phosphate, 1 mg/ml in 10% diethanolamine, pH 9.8, 100 μl/well). The absorbance at 405 nm was quantified by a LabSystem MultiKan reader: color development was in the linear portion of the reaction curve, usually at 15–30 min, which yielded a signal at least 20-fold higher than background.

To determine binding of mutants to the IL-6Rα, increasing amounts of wt IL-6 or mutant IL-6 were added together with the recombinant shIL-6Rα. The mutant receptor binding (expressed as percentage of the wt IL-6) was calculated as the ratio between the amount of wt IL-6 and the amount of mutant IL-6 necessary to displace 50% of recombinant shIL-6Rα bound to coated recombinant hIL-6.

In vivo cell labeling

The establishment of CHO stable transformant clones, constitutively expressing the soluble form of hIL-6Rα (clone CsRh14) and human gp130 (clone CsGh10) was done according to Yasukawa *et al.* (1990 and 1992 respectively). Details of their establishment will be described elsewhere (Sporeno *et al.*, 1994). For *in vivo* labeling, 5×10^6 cells of each clone were incubated with 2 ml methionine-free E-MEM containing 300 μCi/ml [^{35}S]methionine for 4 h at 37°C. The collected supernatants were used as a source of radioactively labeled shIL6-Rα or sgp130 in co-immunoprecipitation experiments.

Immunoprecipitations

Co-immunoprecipitations of sgp130 in the presence of IL-6 and sIL-6Rα with the anti-hIL-6Rα monoclonal were done as described by Yasukawa *et al.* (1992) and Mullberg *et al.* (1993). Basically, 100 μl of CsRh14 conditioned serum-free medium (containing ~10 ng/μl of shIL6-Rα), were incubated with 2 μg of purified anti-hIL6-Rα monoclonal antibody I6R1/9 for 12 h at 4°C. In order to quantify the amount of immunoprecipitated receptor, 40 μl of ^{35}S-labeled shIL-6Rα were added as a tracer.

After addition of 30 μl packed volume of protein A–Sepharose (Pharmacia), incubation was continued for 2 h. The resin was then washed and mixed with 500 μl of labeled soluble human gp130 and different amounts of cold recombinant hIL-6 (see figure legends for details). Following a 12 h incubation at 4°C, immunoprecipitates were washed twice with PBS/0.1% Tween 20 and subjected to SDS–PAGE followed by autoradiography.

Acknowledgements

We thank Drs Lovejoy, Cascio and Eisenberg for making available the coordinates of the bG-CSF structure prior to the PDB release and Tadamitsu Kishimoto for the generous gift of the gp130 cDNA clone. We also thank Anna Tramontano, Maurizio Sollazzo, Antonello Pessi, Riccardo Cortese, Ralph Laufer and Janet Clench for critically reading the manuscript and Yves Cully for artwork.

References

Abdel-Meguid,S.S., Shieih,H.-S., Smith,W.W., Dayringer,H.E., Viland,B.N. and Bentle,L.A. (1987) *Proc. Natl Acad. Sci. USA*, **84**, 6434–6437.

Arcone,R., Pucci,P., Zappacosta,F., Fontaine,V., Malorni,A., Marino,G. and Ciliberto,G. (1991) *Eur. J. Biochem.*, **198**, 541–547.

Bazan,J.F. (1990a) *Immunol. Today*, **11**, 350–354.

Bazan,J.F. (1990b) *Proc. Natl Acad. Sci. USA*, **87**, 6934–6938.

Bazan,J.F. (1991) *Neuron*, **7**, 197–208.

Bernstein,F.C., Koetzle,T.F., Wiliams,G.J.B., Meyer,E.F.,Jr, Brice,M.D., Rodgers,J.R. and Kennard,O. (1977) *J. Mol. Biol.*, **112**, 535–542.

Brakenhoff,J.P.J., Hart,M. and Aarden,L.A. (1989) *J. Immunol.*, **143**, 1175–1182.

Brakenhoff,J.P.J., Hart,M., de Groot,E.R., Di Padova,F. and Aarden,L.A. (1990) *J. Immunol.*, **145**, 561–568.

Brakenhoff,J.P.J., de Hon,F.D., Fontaine,V., Hart,M., de Groot,E.R., Content,J. and Aarden,L.A. (1992) In Revel,M. (ed.), *IL-6: Physiopathology and Clinical Potentials*. Raven Press, New York, pp. 33–41.

Carson,M. (1987) *J. Mol. Graphics*, **5**, 103–106.

Connolly,M.I. (1993) *J. Mol. Graphics*, **11**, 139–141.

Cunningham,B.C. and Wells,J.A. (1989) *Science*, **244**, 1081–1085.

Cunningham,B.C., Ultsch,M., De Vos,A.M., Mulkerrin,M.G., Clauser,K.R. and Wells,J.A. (1991) *Science*, **254**, 821–825.

Davis,S., Aldrich,T.H., Stahl,N., Pan,L., Taga,T., Kishimodo,T., Ip,N.Y. and Yancopolous,G.D. (1993) *Science*, **260**, 1805–1808.

Dayringer,H.E., Tramontano,A., Sprang,S.R. and Fletterick,R.J. (1986) *J. Mol. Graphics*, **4**, 82–87.

Devereux,J., Haeberli,P. and Smithies,O. (1984) *Nucleic Acids Res.*, **12**, 387–395.

De Vos,A.M., Ultsch,M. and Kossiakoff,A.A. (1992) *Science*, **255**, 306–312.

Diedrichs,K., Boone,T. and Karplus,P.A. (1991) *Science*, **254**, 1779–1782.

Fiorillo,M.T., Cabibbo,A., Iacopetti,P., Fattori,E. and Cilberto,G. (1992a) *Eur. J. Immunol.*, **22**, 2609–2615.

Fiorillo,M.T., Toniatti,C., Van Snick,J. and Ciliberto,G. (1992b) *Eur. J. Immunol.*, **22**, 799–804.

Fontaine,V., Savino,R., Arcone,R., De Witt,L., Brakenhoff,J.P.J., Content,J. and Ciliberto,G. (1993) *Eur. J. Biochem.*, **211**, 749–755.

Fuh,G., Cunningham,B.C., Fukunaga,R., Nagata,S., Goeddel,D.V. and Wells,J.A. (1992) *Science*, **256**, 1677–1680.

Gregory,B., Savino,R. and Ciliberto,G. (1994) *J. Immunol. Methods*, in press.

Greenlund,A.C., Schreiber,R.D., Goeddel,D.V. and Pennica,D. (1993) *J. Biol. Chem.*, **268**, 18103–18110.

Hibi,M., Murakami,M., Saito,M., Hirano,T., Taga,T. and Kishimoto,T. (1990) *Cell*, **63**, 1149–1157.

Hill,C.P., Osslund,T.D. and Eisenberg,D. (1993) *Proc. Natl Acad. Sci. USA*, **90**, 5167–5171.

Hirano,T., Akira,S., Taga,T. and Kishimoto,T. (1990) *Immunol. Today*, **11**, 443–449.

Honda,M., Yamamoto,S., Cheng,M., Yasukawa,K., Suzuki,H., Saito,T., Osugi,Y., Tokunaga,T. and Kishimoto,T. (1992) *J. Immunol.*, **148**, 2175–2180.

Hoogenboom,H.R., Griffiths,A.D., Johnson,K.S., Chiswell,D.J., Hudson,P. and Winter,G. (1991) *Nucleic Acids Res.*, **19**, 4133–4137.

Jilka,R.L., Giao,H., Girasole,G., Passeri,G., Williams,D.C., Abrams,J.S., Boyce,B., Broxmeyer,H. and Manolagas,S.C. (1992) *Science*, **257**, 88–91.

Kabsch,W. and Sander,C. (1983) *Biopolymers*, **22**, 2577–2637.

Kishimoto,T., Akira,S. and Taga,T. (1992) *Science*, **258**, 593–597.

Kuga,T., Komatsu,Y., Yamasaki,M., Sekine,S., Miyaji,H., Nishi,T.,

Sato,M., Yokoo,Y., Asano,M., Okabe,M., Morimoto,M. and Itoh,S. (1989) *Biochem. Biophys. Res. Commun.*, **159**, 103–111.
Leebeeck,F.W.G., Kariya,K., Schwabe,M. and Fowlkes,D.M. (1992) *J. Biol. Chem.*, **267**, 14832–14838.
McKay,D.B. (1992) *Science*, **257**, 412–413.
Miyajima,A., Mui,A.L.-F., Ogorochi,T. and Sakamaki,K. (1993) *Blood*, **82**, 1960–1974.
Mullberg,J., Dittrich,E., Graeve,L., Gerhartz,C., Yasukawa,K., Taga,T., Kishimoto,K., Heinrich,P.C. and Rose-John,S. (1993) *FEBS Lett.*, **332**, 174–178.
Murakami,M., Hibi,M., Nakagawa,N., Nakagawa,T., Yasukawa,K., Yamanishi,K., Taga,T. and Kishimoto,T. (1993) *Science*, **260**, 1808–1810.
Nagata,S. and Fukunaga,R. (1991) *Prog. Growth Factor Res.*, **3**, 131–141.
Nishimura,C., Ekida,T., Masuda,S., Futatsugi,K., Itoh,S.-I., Yasukawa,K., Kishimoto,T. and Arata,Y. (1991) *Eur. J. Biochem.*, **196**, 377–384.
Pandit,J., Bohm,A., Jancarik,J., Halenbeck,R., Koths,K. and Kim,S.-H. (1992) *Science*, **258**, 1358–1362.
Powers,R., Garrett,D.S., March,C.J., Frieden,E.A., Gronenborn,A.M. and Glore,G.M (1992) *Science*, **256**, 1673–1677.
Sanger,F., Nicklen,S. and Coulson,A.R. (1977) *Proc. Natl Acad. Sci. USA*, **82**, 5463–5467.
Sauer,U.H., Dao-Pin,S. and Matthews,B. W. (1992) *J. Biol. Chem.*, **267**, 2393–2399.
Savino,R., Lahm,A., Giorgio,M., Cabibbo,A., Tramontano,A. and Ciliberto,G. (1993) *Proc. Natl Acad. Sci. USA*, **90**, 4067–4071.
Senda,T., Shimazu,T., Matsuda,S., Kawano,G., Shimuzu,H., Nakamura,K.T. and Mitsui,Y. (1992) *EMBO J.*, **11**, 3193–3201.
Sporeno,E., Paonessa,G., Salvati,A.L., Graziani,R., Delmastro,P., Ciliberto,G. and Toniatti,C. (1994) *J. Biol. Chem.*, in press.
Studier,F.W. and Moffatt,B.A. (1986) *J. Mol. Biol.*, **189**, 113–130.
Studier,F.W., Rosemberg,A.H., Dunn,J.J. and Dubendorff,J.W. (1990) *Methods Enzymol.*, **185**, 60–89.
Suematsu,S., Matsuda,T., Katsuyuki,A., Akira,S., Nakano,N., Ohno,S., Miyazaki,J., Yamamura,K., Hirano,T. and Kishimoto,T (1986) *Proc. Natl Acad. Sci. USA*, **86**, 7547–7551.
Suematsu,S., Matsusaka,T., Matsuda,T., Ohno,S., Miyazaki,J., Yamamura,K., Hirano,T. and Kishimoto,T. (1992) *Proc. Natl Acad. Sci. USA*, **89**, 232–235.
Taga,T. and Kishimoto,T. (1992) *FASEB J.*, **6**, 3387–3396.
Taga,T., Hibi,M., Hirata,Y., Yamasaki,K., Yasukawa,K., Matsuda,T., Hirano,T. and Kishimoto,T. (1989) *Cell*, **58**, 573–581.
Taga,T., Narazaki,M., Yasukawa,K., Saito,T., Miki,D., Hamaguchi,M., Davis,S., Shoyab,M., Yancopoulos,G.D. and Kishimoto,T. (1992) *Proc. Natl Acad. Sci. USA*, **89**, 10998–11001.
Takeshita,T., Asao,H., Ohtani,K., Ishii,N., Kumaki,S., Tanaka,N., Munakata,H., Nakamura,M. and Sugamura,K. (1992) *Science*, **257**, 379–382.
van Dam,M., Mullberg,J., Schooltink,H., Stoyan,T., Brakenhoff,J.P.J., Graeve,L., Heinrich,P.C. and Rose-John,S. (1993) *J. Biol. Chem.*, **268**, 15285–15290.
Van Snick,J. (1990) *Annu. Rev. Immunol.*, **8**, 253–278.
Vriend,G. (1990) *J. Mol. Graphics*, **8**, 52–56.
Watowich,S.S., Yoshimura,A., Longmore,G.D., Hilton,D.J., Yoshimura,Y. and Lodish,H.F. (1992) *Proc. Natl Acad. Sci. USA*, **89**, 2140–2144.
Yamasaki,K., Taga,T., Yuuichi,H., Yawata,H., Kawanishi,Y., Seed,B., Taniguchi,T., Hirano,T. and Kishimoto,T. (1988) *Science*, **241**, 825–828.
Yasukawa,K., Saito,T., Fukunaga,T., Sekimori,Y., Koishihara,Y., Fukui,H., Ohsugi,Y., Matsuda,T., Yawata,H., Hirano,T., Taga,T. and Kishimoto,T. (1990) *J. Biochem.*, **108**, 673–676.
Yasukawa,K., Futatsugi,K., Saito,T., Yawata,H., Suzuki,M.N.H., Taga,T. and Kishimoto,T. (1992) *Immunol. Lett.*, **31**, 123–130.
Yin,T., Taga,T., Tsang,M.L.-K, Yasukawa,K., Kishimoto,T. and Yang,Y.C. (1993) *J. Immunol.*, **151**, 2555–2561.

Received on December 6, 1993; revised on January 4, 1994